

FREE VIBRATION AND BUCKLING ANALYSIS OF TAPERED BEAM WITH OPEN TRANSVERSE CRACK

A THESIS SUBMITTED IN PARTIAL FULFILLMENT
OF THE REQUIREMENTS FOR THE DEGREE OF

MASTER OF TECHNOLOGY

IN

Structural Engineering

BY

KURAPATI KRISHNA SAGAR

213CE2065



**DEPARTMENT OF CIVIL ENGINEERING
NATIONAL INSTITUTE OF TECHNOLOGY, ROURKELA**

ODISHA, INDIA. 769008

2015

FREE VIBRATION AND BUCKLING ANALYSIS OF TAPERED BEAM WITH OPEN TRANSVERSE CRACK

A THESIS SUBMITTED IN PARTIAL FULFILLMENT
OF THE REQUIREMENTS FOR THE DEGREE OF

MASTER OF TECHNOLOGY

IN

STRUCTURAL ENGINEERING

BY

KURAPATI KRISHNA SAGAR

213CE2065

Under the Guidance of

PROF. Uttam Kumar Mishra



**DEPARTMENT OF CIVIL ENGINEERING
NATIONAL INSTITUTE OF TECHNOLOGY, ROURKELA
ODISHA, INDIA.769008
2013 – 15**



NATIONAL INSTITUTE OF TECHNOLOGY
ROURKELA

CERTIFICATE

*This is to affirm that the thesis entitled, “FREE VIBRATION AND BUCKLING ANALYSIS OF TAPERED BEAM WITH OPEN TRANSVERSE CRACK” submitted by **KURAPATI KRISHNA SAGAR** in partial fulfillment of the requirements for the award of **Master of Technology Degree in Civil Engineering** with specialization in “Structural Engineering” at **National Institute of Technology, Rourkela**, is an authentic work carried out by her under my supervision and guidance.*

To the best of my knowledge, the matter embodied in this thesis has not been submitted to any other university/ institute for award of any Degree or Diploma.

Prof. Uttam Kumar Mishra
Department of Civil Engineering
National Institute of Technology
Rourkela

ACKNOWLEDGEMENT

I am deeply indebted to **Uttam Kumar Mishra**, Assistant Professor, my advisor and guide, for the motivation, guidance, tutelage and patience throughout the research work. I appreciate his broad range of expertise and attention to detail, as well as the constant encouragement he has given me. There is no need to mention that a big part of this thesis is the result of joint work with him, without which the completion of the work would have been impossible.

I express my sincere thanks to **Prof. S. K. Sarangi**, Director of National Institute of Technology, Rourkela and **Prof. S.K. Sahu**, HOD, Department of Civil Engineering for their help and providing the necessary facilities in the department.

I convey my earnest gratitude to Prof. **M. R. Barik**, my faculty and adviser and all faculties Prof. **Pradip Sarkar**, Prof. **A. K. Panda**, Prof. **A. K. Sahoo**, Prof. **K. C. Biswal** and Prof. **Asha Patel** for their help in settling down in the first year. I also thank Prof. **A. V. Asha**, PG Coordinator, for providing suitable slots during the presentation and Viva.

Thanks to Rakesh Chanamala, Indrajeeth M S and B Rohini for making joyful learning here. Finally, I owe my heartiest gratitude to my father Janardhan Rao, mother Yashoda, my sister Dr. Priyanka and brother Rahul Krishna for their unconditional support, love, inspiration and sacrifices.

KURAPATI KRISHNA SAGAR

Abstract

Tapering beams are used in diversities for their economic, aesthetic and other considerations in architecture, aeronautics, robotics and other innovative engineering applications. More recently they have been the subject of numerous studies. Present study deals with the vibration and buckling behavior of linearly tapered beams with single open transverse cracks. The variety of natural frequency and buckling load with distinctive parameters including relative crack depth, position of cracks and the slope of the beam are analyzed using finite element methods (FEM). A Matlab code is developed for the computation of natural frequencies and buckling loads of the cracked beam. Crack in the beam is represented by a rotating spring in line with T. D. Chaudhari, S. K. Maiti (1999). Stiffness matrix of the cracked tapered beam element is obtained from the flexibility matrix of the intact beam and the additional flexibility matrix due to crack. Free vibration frequencies and buckling load of a cracked cantilever beam reduce with an increase in crack depth. And also frequencies reduce more with the crack located nearer to the fixed end than the free end. For an intact tapered beam the frequencies vary more for the depth ratio compared to breadth ratio. The free vibration frequencies of a single cracked beam also vary more for depth ratio compared to breadth ratio. The vibration results can also be utilized as a tool for structural health monitoring, testing of structural integrity, execution and safety.

Keywords: tapered beam, natural frequency, buckling, FEM, crack etc.

Table of Contents

ACKNOWLEDGEMENT	ii
Abstract	iii
LIST OF FIGURES	vi
LIST OF TABLES	vii
1. INTRODUCTION	3
1.1. Introduction	3
2. LITERATURE REVIEW	4
2.1. Introduction	4
2.2. Literature Review	4
2.3. Objective and Scope of the Present Investigation	8
3. THEORITICAL MODELLING OF A TAPERED BEAM	9
3.1. Linearly Tapered Beam Element	9
3.2. Governing Differential Equations of motion of Tapered Beam	11
4. FINITE ELEMENT FORMULATION	13
4.1. Introduction	13
4.1. Calculation of Shape Function:	14
4.2. Stiffness Calculation of Tapered Beam:	16
4.3. Mass Matrix of Tapered Beam	19
4.4. Buckling Theory	20
4.5. Mathematical Formulation for Crack Stiffness	21
5. RESULTS AND DISCUSSION:	25
5.1. Introduction:	25
5.2. Numerical Problem for Intact Tapered Beam:	25
5.2.1. Convergence Study	26
5.2.2. Comparison with Previous Studies:	27
5.2.3. Effect of Taper Ratio on Frequency for an intact tapered beam:	27
5.3. Effect depth ratio on buckling load for an intact tapered beam:	28
5.4. Numerical Problem for Tapered Beam with Single Transverse Crack:	29
5.4.1. Convergence study:	30
5.4.2. Comparison with Previous Studies:	31

5.4.3.	Effect of Crack on frequencies at Various Locations in Tapered Beam for Fixed-Free Boundary Condition	33
5.4.4.	Effect of Taper Ratio on Frequency of a single cracked tapered beam:	36
5.5.	Buckling of beam subjected to single crack for different end conditions of the beam.....	37
5.5.1.	Fixed free beam:	38
5.5.2.	Hinged-Hinged beam:	39
5.5.3.	Fixed–Fixed beam	40
5.5.4.	Fixed-Hinged beam	41
5.6.	Effect taper ratio on buckling load of a single cracked tapered beam:	42
6.	CONCLUSION AND FUTURE WORK	44
6.1.	Conclusion.....	44
6.2.	Scope of the Future Work.....	45
REFERENCES.....		46

LIST OF FIGURES

Figure 3-1 Different shapes of cross section of tapered beam with corresponding shape factors	10
Figure 4-1 Schematic diagram of a tapered beam element with 2 degrees of freedom per node	14
Figure 4-2 A regular cracked beam element which is subjected to shearing force and bending moment of rectangular cross-section area.....	21
Figure 5-1 Convergence of fundamental frequency of an intact tapered cantilever beam	26
Figure 5-2 Effect of α on frequency for constant values of β	27
Figure 5-3 Effect of β on frequency for constant values of α	28
Figure 5-4 Effect depth ratio on buckling load	29
Figure 5-5 Geometrical representation of crack.....	30
Figure 5-6 Convergence of fundamental frequency of a single cracked tapered cantilever beam.....	31
Figure 5-7 Variation of first mode natural frequency of cracked tapered cantilever beam for different values of χ and a/h_c	33
Figure 5-8 Variation of second mode natural frequency of cracked tapered cantilever beam for different values of χ and a/h_c	34
Figure 5-9 Variation of third mode natural frequency of cracked tapered cantilever beam for different values of χ and a/h_c	35
Figure 5-10 Variation of fourth mode natural frequency of cracked tapered cantilever beam for different values of χ and a/h_c	36
Figure 5-11 Effect of β on frequency for constant values of α	36
Figure 5-12 Effect of β on frequency for constant values of α	37
Figure 5-13 Variation of non-dimensional buckling load (P_c/P_i) with respect to relative location of crack (L_1/l) for different relative crack depths for Fixed-Free beam.....	38
Figure 5-14 Variation of non-dimensional buckling load (P_c/P_i) with respect to relative location of crack (L_1/l) for different relative crack depths for Hinged-Hinged beam.....	39
Figure 5-15 Variation of non-dimensional buckling load (P_c/P_i) with respect to relative location of crack (L_1/l) for different relative crack depths for Fixed-Fixed beam	40
Figure 5-16 Variation of non-dimensional buckling load (P_c/P_i) with respect to relative location of crack (L_1/l) for different relative crack depths for Fixed-Hinged beam	41
Figure 5-17 Effect of taper ratio on buckling load for single cracked tapered beam	43

LIST OF TABLES

Table 5-1 Comparison of frequencies of an intact tapered cantilever beam with previous studies	27
Table 5-2 Comparison of natural frequencies of a single cracked tapered cantilever beam with previous studies	32
Table 5-3 Comparison of frequencies with previous studies for different values of crack depth and location	32

NOMENCLATURE

Description	Symbols
Moment of inertia at the fixed end	I_o
Moment of inertia at the free end	I_l
Width of the beam at the fixed end	b_o
Width of the beam at the free end	b_l
Depth of the beam at the fixed end	h_o
Depth of the beam at the free end	h_l
Cross-sectional area at length x from free end	A_x
Dimensionless number $(h_o/h_l)-1$	R
Element stiffness matrix	$[K^e]$
Consistent mass matrices	$[M^e]$
Nodal degree of freedom vector	d^e
Hermitian shape function	$H_i(x)$
Natural frequency	Ω
h_o/h_l	A
b_o/b_l	B
Mode shape vector	$\{\phi\}$
Element domain	Ψ^e
The number of elements for the beam	n

Dedicated to
My beloved Parents
Mr. JANARDHAN RAO
Mrs. YASHODA

INTRODUCTION

1.1. Introduction

It is known that beams are the basic structural components and can be classified according to their geometric configuration. They are usually uniform or non-uniform, and slender or thick. Non-prismatic members are increasingly being used in diversities as for their economic, aesthetic, and other considerations. If we analyze the non-uniform beams more practically provide a better or more suitable distribution of mass and strength than uniform beams and therefore can meet special functional requirements in architecture, aeronautics, robotics, and other innovative engineering applications and they have been the subject of numerous studies. Tapered beam have functions in turbine machinery. For long spans, tapered beams are the alternatives for uniform beams, which give economically good results.

The design of the structures to resist dynamic forces, such as wind and earthquakes, requires knowledge of their natural frequencies and the mode shapes of vibration. Identification of defects like crack in a beam from the vibration pattern is a subject of interest for many researchers. Present study enables possible detection of the crack based on the measurement of natural frequencies. In this study modeling of a tapered beam of linearly variable depth and constant thickness with crack normal to the axis is performed by FEM in Matlab environment.

LITERATURE REVIEW

2.1. Introduction

Many engineering structures may have structural defects such as cracks due to mechanical vibrations, environmental attack, corrosion, long term service and cyclic load etc. A crack on a beam element introduces local flexibility due to strain energy concentrations in the vicinity of the crack tip under the load. This flexibility changes the dynamic behavior of the beam. The dynamic characteristics of cracked beams are of considerable importance in many designs.

2.2. Literature Review

Wang and Worley (1966) gave a report on tables of natural frequencies and nodes for transverse vibration tapered beams by considering the cross sectional area bounded by a curve

$\left(\frac{y}{h}\right)^\beta + \left(\frac{z}{b}\right)^\gamma = 1$, h & b are the thickness and width varying along the beam according to the

relations, $h = h_0 \left(\frac{x}{l}\right)^\phi$, $b = b_0 \left(\frac{x}{l}\right)^\psi$ Where, β , γ and ϕ are the positive constants not necessarily

integers. **Gupta (1985)** derived the stiffness and consistent mass matrices for tapered beam with linearly variable cross-sectional elements in explicit form. He derived expression for any type of cross sectional area. He obtained Numerical results of free vibration for some tapered beams using the derived matrices. These obtained results are compared with the analytic solution of uniform beam elements. Convergence characteristics and solution accuracy are examined. **Rosa and Auciello (1996)** examined the dynamic behavior of tapered beams with variable cross-

section. He considered the ends of the beams to be flexible both rotationally and axially. For this, they used Bessel functions for solving equation of motion. When they applied boundary conditions, the equation obtained is a function of four flexibility functions. The cross sectional parameters such as height and depth are linearly varied. **Chaudhari and Maiti (1999)** proposed the transverse vibration of the tapered beam with constant thickness and linearly variable depth with an 'open' edge crack present normal to its axis. They introduced the concept of rotational spring to represent the crack section. The Frobenius method was used to detect the possible location of the crack. A number of numerical examples are discussed to show the effectiveness of the inverse problem. Crack sizes varying from 10-15% of depth have been examined. **Bazoune et. al. (2001)** used the finite element method to develop a method for dynamic response of spinning tapered Timoshenko beam. They considered the effects of Coriolis forces, rotary inertia, shear deformation, angular setting, taper ratios and hub radius of the beam while developing the equations of motion. The values obtained by this method are less accurate. **Radhakrishnan (2004)** studied the resonance response of a cracked cantilever beam of rectangular cross section. The method is based on fracture mechanics quantities like stress intensity factor, strain energy release rate, and compliance. With the increase in crack length the fundamental frequency decreases, thus stiffness also decreases. They showed that when the amplitude of vibration increases the natural event of resonance gets shifted with increase in length of the crack. **Behzad et. al. (2005)** developed the equations of motion with the corresponding boundary conditions for free bending vibration of a beam in the presence of an open edge crack. They used the Hamilton principle for this implementation. The crack has been demonstrated as a continuous disturbance function in displacement field which could be acquired from fracture mechanics. **Daniel J. Marquez-Chisolm (2006)** presented the torsion response

and dynamic nonlinear bending of a cantilever beam. The natural frequencies are measured in the flatwise and edgewise headings at diverse static root pitch angles with differing levels of tip weights. The deliberate natural frequencies were contrasted with linear equations of motion, a nonlinear computer model and past tests to confirm the nonlinear effects of root pitch angle and tip weights. **Kukla and Zamojska (2006)** applied green's function method to a free vibration problem of a system of non-uniform beams coupled with non-homogeneous elastic layers. The frequency equation is obtained by using a quadrature rule of a Newton-Cotes type. **Mazanoglu et. al. (2008)** paper presented the energy-based method for the vibration identification of non-uniform Euler-Bernoulli beams having different open cracks. The dissemination of energy expended is dictated by considering the both strain change at the cracked beam surface and extensive impact of the stress field created by the angular displacement of the beam because of bending. The Rayleigh-Ritz approximation strategy is utilized as a part of the analysis. They discussed about the impact of vibration amplitude on the nonlinear frequency. **Karaagac et. al. (2009)** examined the effects of crack ratios and positions on the fundamental frequencies and buckling loads of slender cantilever Euler beams with a single edge crack both experimentally and numerically utilizing the finite element method, based on energy approach. The administering matrix equations are gotten from the standard and cracked beam elements joined with the local flexibility concept. The analyses are directed utilizing examples having edge cracks of distinctive depths at diverse positions to accept the obtained numerical results. **Rezaee and Hassannejad (2010)** proposed energy balance method for free vibration analysis of cracked cantilever by considering both the damping due to the crack and structural damping. The stiffness changes in the crack location are thought to be a nonlinear amplitude dependent function which causes the frequencies and mode shapes of the beam to change constantly with

time. **Bayat *et. al.* (2010)** published their journal on analytical study of tapered beam vibration frequencies. The considered represents the governing equation of the nonlinear, extensive amplitude free vibrations of tapered beams. They actualized another system called Homotopy Perturbation Method (HPM) over the antiquated Chinese technique called the Max-Min Approach (MMA). **Cheng *et. al.* (2011)** studied the vibration characteristics of the cracked rotating tapered beam are explored by the p-version finite element method. The shape functions enhanced with the shifted Legendre orthogonal polynomials are employed to represent the transverse displacement field within the rotating tapered beam element. The crack element stiffness matrix and the p version finite element model of the basic framework are gotten by utilizing fracture mechanics and the Lagrange equation, respectively. The impacts of crack location, crack size, rotating speed and hub radius on vibration qualities of a cracked rotating tapered beam are investigated. **Achawakorn and Jearsiripongkul (2012)** introduced an approximate method to analyze uniform and non-uniform beam. Euler-Bernoulli thin beam equation is the base of the differential equation formation. This analytical method gives approximate results at the highest degree of calculations. Galerkin's method is used in this analysis. **Auciello (2013)** analyzed the free vibration characteristics of rotating tapered Rayleigh beam. He proposed two approaches to the dynamic analysis of rotating beam. One is discretization "CDM" method and the other is a vocational Rayleigh–Ritz like method. The parameters for the hub radius, rotational speed and taper ratio are incorporated. **Jawad (2013)** studied the free vibration and buckling behavior of a non-uniform Euler-Bernoulli beam under various degrees of flexural bending and tapered parameter. His studies concluded that the natural frequency and buckling load decrease with increasing the tapered parameter and degree of flexural stiffness of tapered beams. **Trahair (2014)** analyzed the the elastic in-plane bending and

out of-plane buckling of indeterminate beam structures whose members are having tapered and of mono-symmetric I cross-section with efficient finite element method. Tapered finite element formulations are created by numerical integration rather than the closed forms. The common approximation in which tapered elements are supplanted by uniform elements is indicated to converge gradually, and to prompt off base forecasts for tapered mono-symmetric beams.

2.3.Objective and Scope of the Present Investigation

As per review of the previous literature, no work was done in the field of parametric study of the free vibration and buckling analysis of the tapered beam by finite element analysis. Hence present study mainly focused on,

- Free vibration study of a tapered cantilever beam with and without a transverse open crack.
- To study the buckling of a tapered beam in the presence of a single edge crack normal to the axis.
- The influence of various geometric features like taper ratio, crack length and location of the crack, etc. on the free vibrations and static stability to be investigated analytically.

THEORITICAL MODELLING OF A TAPERED BEAM

3.1. Linearly Tapered Beam Element

The beam element is assumed to be associated with two degrees of freedom, one rotation and one translation at each node. The location and positive directions of these displacements in a linearly varying tapered beam element are demonstrated in fig below. Some commonly utilized cross-sectional shapes of beams are demonstrated in Table. The depths of the cross sections at the ends are represented by h_1 (at fixed end) and h_2 (at free end), similarly the widths at the ends are represented by b_1 (at fixed end) and b_2 (at free end) respectively. Length of the beam is taken as 'l'. The axis about which bending is assumed to occur is demonstrated by a line in the center coinciding with the neutral axis.

In most of the cases, the variation in cross-sectional area along the length is taken from the accompanying equation,

$$A_x = A_l \left[1 + r \frac{x}{l} \right]^m \quad (3.1)$$

And the variation in moment of inertia along the length is represented by the following equation,

$$I_x = I_l \left[1 + r \frac{x}{l} \right]^n \quad (3.2)$$

Where,

$$r = \frac{h_o}{h_l} - 1 \quad (3.3)$$

A_x , I_x are the cross sectional area and the moment inertia at a distance x from the smaller end.

Here, m and n are the shape factors that are depending on the shape of the cross section and the dimension of the beam. The shape factors can be assessed theoretically by the Eq. 3.1 and 3.2.

As we apply the boundary conditions for the beam, $A_x=A_o$ and $I_x=I_o$ at $x=l$, which results the following equation,

$$m = \frac{\ln \left[\frac{A_o}{A_l} \right]}{\ln \left[\frac{h_o}{h_l} \right]}, \quad n = \frac{\ln \left[\frac{I_o}{I_l} \right]}{\ln \left[\frac{h_o}{h_l} \right]} \quad (3.4)$$

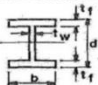
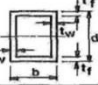
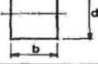
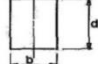
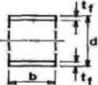
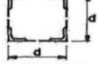
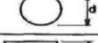
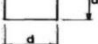
Shape (1)	Shape Factors		Category (4)
	n (2)	m (3)	
 Wide-flange or I-section Constant dimensions b , t_w , t_f Varying depth d Bending about horizontal axis	2.1 to 2.6	varies	1
 Closed box section Constant dimensions b , t_w , t_f Varying depth d Bending about horizontal axis	2.1 to 2.6	varies	
 Solid, rectangular section Constant width b Varying depth d Bending about horizontal axis	3	1	2
 Solid, rectangular section Constant width b Varying depth d Bending about vertical axis	1	1	3
 Open-web section Constant dimensions b , t_f Varying depth d Bending about horizontal axis	2	0	4
 Tower section Constant areas concentrated near corners Varying dimension d	2	0	
 Solid, circular section Varying diameter d	4	2	5
 Solid, square section Varying dimension d	4	2	

Figure 3-1 Different shapes of cross section of tapered beam with corresponding shape factors ^[11]

Consequently, the shape factors can be found effectively regardless of the cross-section using the dimensions of at the ends. Calculation of shape factors (m and n) from Eq. 3.4 uncovers that the expressions for A_x and I_x are definite at both ends of the beam. At times

concerning beams of I-section (fig. 3.1), it has been found that, at points in the middle of along the beam, A_x and I will go amiss somewhat from the true values. The degree of this deviation is very little and for beams of every single normal extent, Eq. 3.1 and 3.2 gives estimations of the area and moment of inertia at each section along the beam inside of one percent of deviation, which can be disregarded, of the true values. The dimensionless shape factors m, n varies in between 2.2 -2.8.

For the following theoretical analysis a rectangular beam with a linear variable width and depth is considered.

3.2. Governing Differential Equations of motion of Tapered Beam

A general Euler's Bernoulli beam is assumed which is tapered both in horizontal as well as vertical linearly.

$$\frac{\partial^2}{\partial x^2} \left(EI_x \frac{\partial^2 y}{\partial x^2} \right) + \frac{\rho A_x}{g} \left(\frac{\partial^2 y}{\partial t^2} \right) = 0 \quad (3.5)$$

The width and depth vary linearly given by,

$$\begin{aligned} h &= h_l + (h_o - h_l)(x/l) \\ b &= b_l + (b_o - b_l)(x/l) \end{aligned} \quad (3.6)$$

The corresponding area and moment of inertia varying accordingly,

$$\begin{aligned} A(x) &= [b_l + (b_o - b_l)(x/l)][h_l + (h_o - h_l)(x/l)] \\ I(x) &= \frac{1}{12} [b_l + (b_o - b_l)(x/l)][h_l + (h_o - h_l)(x/l)]^3 \end{aligned} \quad (3.7)$$

All the expressions for the beam area and moment of inertia at any cross-section are composed in the wake of considering the variance along the length to be linear. So, here, L is the length of the beam, E is the young's modulus, or modulus of elasticity, I is the moment of inertia of the beam, ρ is the weight density, A is the area, ' $\rho A/g$ ' together gives mass per unit length.

Since we are considering only free vibration, the motion will be of the form $y(x,t) = z(x) \sin(\omega t)$

$$\frac{\partial^2}{\partial x^2} \left(EI_x \frac{\partial^2 z}{\partial x^2} \right) = \frac{\rho A_x}{g} (\omega^2 z) \quad (3.8)$$

$$\begin{aligned} & \frac{d^4 z}{du^4} + \frac{2d^3 z}{du^3} \left[\frac{(b_o - b_l)}{b_l + (b_o - b_l)u} + \frac{3(h_o - h_l)}{h_l + (h_o - h_l)u} \right] + \frac{6d^2 z}{du^2} \left[\frac{(b_o - b_l)(h_o - h_l)}{[b_l + (b_o - b_l)u][h_l + (h_o - h_l)u]} + \frac{(h_o - h_l)^2}{[h_l + (h_o - h_l)u]^2} \right] \\ & = \frac{12I^4 \Omega^2}{Eg} \left[\frac{1}{[h_l + (h_o - h_l)u]} \right]^3 z \end{aligned} \quad (3.9)$$

By proper approximation i.e. $\alpha = \frac{h_o}{h_1}$ and $\beta = \frac{b_o}{b_1}$ and $k = \frac{12\rho\omega^2}{Egh_1}$ the above equations get

transformed to,

$$\begin{aligned} & \frac{d^4 z}{du^4} + \frac{2d^3 z}{du^3} \left[\frac{(\beta - 1)}{1 + (\beta - 1)u} + \frac{3(\alpha - 1)}{1 + (\alpha - 1)u} \right] + \frac{6d^2 z}{du^2} \left[\frac{(\beta - 1)(\alpha - 1)}{[1 + (\beta - 1)u][1 + (\alpha - 1)u]} + \frac{(\alpha - 1)^2}{[1 + (\alpha - 1)u]^2} \right] \\ & = \left[\frac{(lk)^2 z}{[1 + (\alpha - 1)u]^2} \right] \end{aligned} \quad (3.10)$$

Eq. 3.10 is the final equation of motion of a rectangular beam with a double - tapered cross-section. It is then solved by numerical integration to give values of 'lk' for various values of taper ratios for beam with a clamped-free boundary conditions.

i.e, at $x=0$ or $u=0$, $z=0$ and $\frac{d^2 z}{du^2} = 0$

At $x=1$ or $u=1$, $z=0$ and $\frac{dz}{du} = 0$

Then we get $\omega = k^2 h_l \sqrt{\frac{Eg}{12\rho}}$

The relation can be utilized as an examination while comprehending with FEA to demonstrate the impact of taper ratio on fundamental frequencies and mode shapes.

FINITE ELEMENT FORMULATION

4.1. Introduction

Finite element method is the most suitable technique for digitalized computers. It includes a body to be discretized into smaller bodies having equivalent system. Then the whole body is represented by assembling such small bodies. Every subsystem is comprehended separately and the outcomes so acquired are then joined to get solution for the entire body. The finite element method is relevant to the extensive variety of problems, including nonlinear stress-strain relations, non-homogeneous materials and confounded boundary conditions. Such problems are typically handled by one of the three methodologies, namely,

(1). Displacement Method or Stiffness Method

(2). Equilibrium Method or Force Method

(3). Mixed Method

Our concern is particularly on Displacement method, is widely used method because of the simplicity and can handled easily with a computer.

In stiffness method approach a body partitioned into a number of finite elements and these elements are interconnected at the joints called as 'Nodes'. The displacements in each element are represented by simple functions. The obscure magnitudes of these functions are the displacements or the displacement derivatives at the nodes. A displacement function is usually expressed as a polynomial.

A polynomial function should possess the following requirements,

1. It is to be continuous within the elements and should be compatible between the adjacent elements.
2. It should include the rotations and rigid body displacements of the element.
3. Should possess a strained state that is consistent.

4.1. Calculation of Shape Function:

The tapered beam element is assumed to be with two degrees of freedom, one rotation and one translation at each node, as shown in figure 4-1.

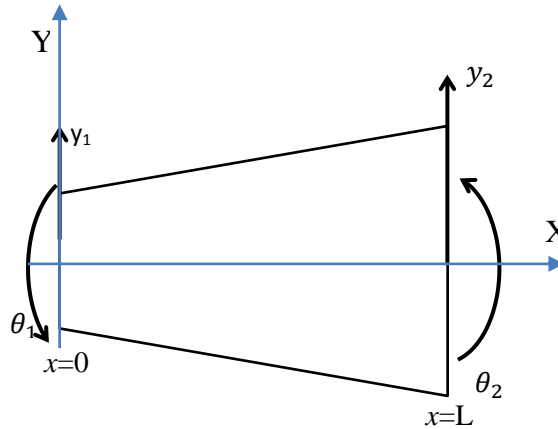


Figure 4-1 Schematic diagram of a tapered beam element with 2 degrees of freedom per node

The Euler-Bernoulli beam equation is in view of the presumption that the plane normal to the neutral axis before deformation remains normal to the neutral axis after deformation. Since the beam is having 4 nodal variables, hence a cubic polynomial function $y(x)$ is assumed as,

$$y(x) = a_0 + a_1x + a_2x^2 + a_3x^3 \quad (4.1)$$

The slope can be computed, from the assumptions made for Euler-Bernoulli beam as,

$$\theta(x) = a_1 + 2a_2x + 3a_3x^2 \quad (4.2)$$

Where a_0, a_1, a_2, a_3 are constants. Eq.4.1 can be written as,

$$Y(x) = \begin{bmatrix} 1 & x & x^2 & x^3 \end{bmatrix} \begin{bmatrix} a_0 \\ a_1 \\ a_2 \\ a_3 \end{bmatrix}$$

$$\therefore Y(x) = [C][a] \quad (4.3)$$

$$[C] = \begin{bmatrix} 1 & x & x^2 & x^3 \end{bmatrix} \text{ and } [a] = \begin{bmatrix} a_0 \\ a_1 \\ a_2 \\ a_3 \end{bmatrix} \quad (4.4)$$

Where,

For convenient local coordinate system is taken $x_1=0, x_2=1$ that leads to,

$$y_1 = a_0;$$

$$\theta_1 = a_1;$$

$$y_2 = a_0 + a_1l + a_2l^2 + a_3l^3;$$

$$\theta_2 = a_1 + 2a_2l + 3a_3l^2;$$

In a matrix representation, this can be written as,

$$\begin{bmatrix} y_1 \\ \theta_1 \\ y_2 \\ \theta_2 \end{bmatrix} = \begin{bmatrix} 1 & 0 & 0 & 0 \\ 0 & l & 0 & 0 \\ 1 & l & l^2 & l^3 \\ 0 & 1 & 2l & 3l^2 \end{bmatrix} \begin{bmatrix} a_0 \\ a_1 \\ a_2 \\ a_3 \end{bmatrix} \quad (4.6)$$

$$[\alpha] = [A][a]$$

$$\therefore [a] = [A]^{-1} [\alpha] \quad (4.7)$$

Substituting above value in Eq. 4.3, we get

$$Y(x) = [C][A]^{-1} [\alpha] \quad (4.8)$$

$$Y(x) = [H][\alpha]$$

$$[H] = [C][A]^{-1}$$

$$\text{Here, } [A]^{-1} = \begin{bmatrix} 1 & 0 & 0 & 0 \\ 0 & l & 0 & 0 \\ \frac{-3}{l^2} & \frac{-2}{l} & \frac{3}{l^2} & \frac{-1}{l} \\ \frac{2}{l^3} & \frac{1}{l^2} & \frac{-2}{l^3} & \frac{-1}{l^2} \end{bmatrix}; \quad (4.9)$$

$$[H] = [H_1(x) \ H_2(x) \ H_3(x) \ H_4(x)]$$

Here, $H_i(x)$ called as Hermitian shape function,

$$H_1(x) = 1 - \frac{3x^2}{l^2} + \frac{2x^3}{l^3}, \ H_2(x) = x - \frac{2x^2}{l} + \frac{x^3}{l^2}$$

$$H_3(x) = \frac{3x^2}{l^2} - \frac{2x^3}{l^3}, \ H_4(x) = -\frac{x^2}{l} + \frac{x^3}{l^2}$$

4.2. Stiffness Calculation of Tapered Beam:

The Euler-Bernoulli equation for bending of the beam is,

$$\frac{\partial^2}{\partial x^2} \left(EI \frac{\partial^2 y}{\partial x^2} \right) + \rho A \left(\frac{\partial^2 y}{\partial t^2} \right) = q(x, t) \quad (4.10)$$

Where, $y(x, t)$ is the displacement of the beam in transverse direction, EI is the rigidity of the beam, ρ is the mass density and $q(x, t)$ is the external pressure loading, x and t represents the

spatial and time axis along the beam axis. We apply Galerkin's method or Weighted residual method to the above beam equation to develop the finite element formulation. The average weighted residual of Eq 4.10 is

$$I = \int_0^l \left(\rho \frac{\partial^2 y}{\partial t^2} + \frac{\partial^2}{\partial x^2} \left(EI(x) \frac{\partial^2 y}{\partial x^2} \right) - q \right) p dx = 0 \quad (4.11)$$

Where p is the test function and l is the length of the beam. The weak formulation of the Eq.4.11 can be obtained by integrating by parts twice for the second term of the equation. By allowing the discretization of the beam into a finite number of elements gives,

$$I = \sum_{i=1}^n \left[\int_{\psi^e} \rho \frac{\partial^2 y}{\partial x^2} p dx + \int_{\psi^e} EI(x) \frac{\partial^2 y}{\partial x^2} \frac{\partial^2 p}{\partial x^2} dx - \int_{\psi^e} q p dx \right] + \left[-Vp - M \frac{dp}{dx} \right]_0^l = 0 \quad (4.12)$$

Where,

$$V = -EI(x) \frac{\partial^3 y}{\partial x^3}, \text{ is the shear force,}$$

$$M = -EI(x) \frac{\partial^2 y}{\partial x^2}, \text{ is the bending moment,}$$

Ψ^e is element domain and 'n' is the number of elements of the beam.

Applying the Hermitian shape function and the Galerkin's method to the second term of the Eq.4.12 brings about the stiffness matrix of the tapered beam element with rectangular cross section..i.e,

$$[K]^e = \int_0^l [B]^T EI(x) [B] dx \quad (4.13)$$

Where,

$$[B] = \begin{bmatrix} H_1'' & H_2'' & H_3'' & H_4'' \end{bmatrix} \quad (4.14)$$

And, nodal degree of freedom for the corresponding element is,

$$\{d^e\} = \{y_1 \quad \theta_1 \quad y_2 \quad \theta_2\}^T \quad (4.15)$$

In eq (4.14) double prime indicates the second derivative of the function.

Since we assumed the beam to be homogeneous and isotropic, the modulus of elasticity, E can be considered as constant and taken out from the integration, then the eq 4.13 becomes,

$$K^e = E \begin{bmatrix} k_{11} & k_{12} & k_{13} & k_{14} \\ k_{21} & k_{22} & k_{23} & k_{24} \\ k_{31} & k_{32} & k_{33} & k_{34} \\ k_{41} & k_{42} & k_{43} & k_{44} \end{bmatrix} \quad (4.16)$$

$$k_{mn} = k_{nm} = E \int_0^l I(x) \frac{\partial^2 H_m}{\partial x^2} \frac{\partial^2 H_n}{\partial x^2} dx \quad (4.17)$$

Where k_{mn} ($m, n = 1, 4$) are the coefficients of the element stiffness matrix.

By solving the above equation, we get the respective values of coefficients of the element stiffness matrix for the beam of rectangular cross-section,

$$[K^e] = E \begin{bmatrix} \frac{6(I_o + I_l)}{l^3} & \frac{2(I_o + 2I_l)}{l^2} & -\frac{6(I_o + I_l)}{l^3} & \frac{2(2I_o + I_l)}{l^2} \\ \frac{2(I_o + 2I_l)}{l^2} & \frac{I_o + 3I_l}{l} & -\frac{2(I_o + 2I_l)}{l^2} & \frac{I_o + I_l}{l} \\ -\frac{6(I_o + I_l)}{l^3} & -\frac{2(I_o + 2I_l)}{l^2} & \frac{6(I_o + I_l)}{l^3} & -\frac{2(2I_o + I_l)}{l^2} \\ \frac{2(2I_o + I_l)}{l^2} & \frac{I_o + I_l}{l} & -\frac{2(2I_o + I_l)}{l^2} & \frac{3I_o + I_l}{l} \end{bmatrix} \quad (4.18)$$

Eq. 4.18 is the element stiffness matrix for rectangular cross sectioned tapered beam.

4.3. Mass Matrix of Tapered Beam

Since, for dynamic analysis of beams, inertia force needs to be incorporated. In this case, transverse deflection is a function of x and t . The deflection is represented within a beam component is given underneath,

$$y(x, t) = H_1(x)y_1(t) + H_2(x)\theta_2(t) + H_3(x)y_3(t) + H_4(x)\theta_4(t) \quad (4.19)$$

$$M^e = \rho \begin{bmatrix} m_{11} & m_{12} & m_{13} & m_{14} \\ m_{21} & m_{22} & m_{23} & m_{24} \\ m_{31} & m_{32} & m_{33} & m_{34} \\ m_{41} & m_{42} & m_{43} & m_{44} \end{bmatrix} \quad (4.20)$$

$$m_{mn} = m_{nm} = \int_0^l A(x)[H]^T [H] dx \quad (4.21)$$

Where m_{mn} ($m, n = 1, 4$) are the coefficients of the element mass matrix.

$$[M^e] = \rho \begin{bmatrix} \frac{l(10A_l + 3A_o)}{35} & \frac{l^2(15A_l + 7A_o)}{420} & \frac{9l(A_l + A_o)}{140} & \frac{-l^2(7A_l + 6A_o)}{420} \\ \frac{l^2(15A_l + 7A_o)}{420} & \frac{l^3(5A_l + 3A_o)}{840} & \frac{l^2(6A_l + 7A_o)}{420} & \frac{-l^3(A_l + A_o)}{280} \\ \frac{9l(A_l + A_o)}{140} & \frac{l^2(6A_l + 7A_o)}{420} & \frac{l(3A_l + 10A_o)}{35} & \frac{-l^2(7A_l + 15A_o)}{420} \\ \frac{-l^2(6A_l + 7A_o)}{420} & \frac{-l^3(A_l + A_o)}{280} & \frac{-l^2(7A_l + 15A_o)}{420} & \frac{l^3(3A_l + 5A_o)}{840} \end{bmatrix} \quad (4.22)$$

The equation of motion for the beam can be written as

$$[M]\{\ddot{u}\} + [K]\{d\} = 0 \quad (4.23)$$

For free vibration analysis equation implies,

$$(\omega^2[M] + [K])\{\phi\}e^{i\omega t} = 0 \quad (4.24)$$

Where, ω is the natural frequency of motion and $\{\phi\}$ is mode shape (Eigen vector).

Using the above equation of motion of the free vibration the mode shapes and frequency can be easily calculated.

4.4. Buckling Theory

The equation of motion in matrix form for the vibration of a beam under load is written as,

$$[M]\{\ddot{q}\} + [[K] - P[K_g]]\{q\} = 0 \quad (4.25)$$

Where, [M] = Consistent mass matrix,

[K] = Bending stiffness matrix of the beam,

[K_g] = geometric stiffness matrix,

{q} = displacement load,

P = External force vector

For static stability,

$$[[K_e] - P_{cr}[K_g]]\{q\} = 0 \quad (4.26)$$

Where,

$$K_g = P_{cr} \begin{bmatrix} k_{g11} & k_{g12} & k_{g13} & k_{g14} \\ k_{g21} & k_{g22} & k_{g23} & k_{g24} \\ k_{g31} & k_{g32} & k_{g33} & k_{g34} \\ k_{g41} & k_{g42} & k_{g43} & k_{g44} \end{bmatrix} \quad (4.27)$$

$$k_{gmn} = k_{gnm} = E \int_0^l P_{cr} \frac{\partial H_m}{\partial x} \frac{\partial H_n}{\partial x} dx \quad (4.28)$$

Where, m_{mn} ($m, n = 1, 4$) are the coefficients of the geometric stiffness matrix

$$[K_g] = \frac{1}{30L_e} \begin{bmatrix} 36 & 3L_e & -36 & 3L_e \\ 3L_e & 4L_e^2 & -3L_e & L_e^2 \\ -36 & -3L_e & 36 & -3L_e \\ 3L_e & -L_e^2 & -3L_e & 3L_e^2 \end{bmatrix} \quad (4.29)$$

4.5. Mathematical Formulation for Crack Stiffness

A regular cracked uniform cantilever beam element of the rectangular cross sectional area with 'b' as the breadth, 'h' as the depth of the beam and the depth of the crack are indicated by 'a' as shown in fig.4.2.

The left side end, which is fixed, is denoted with node 'i' and right side node is denoted with 'j'. A shearing force ' P_1 ' and bending moment ' P_2 ' is subjected by the beam element. The overseeing equations of the vibration analysis of the uniform beam with open transverse crack are processed on the premise of the FEM model proposed by Zheng(2004).

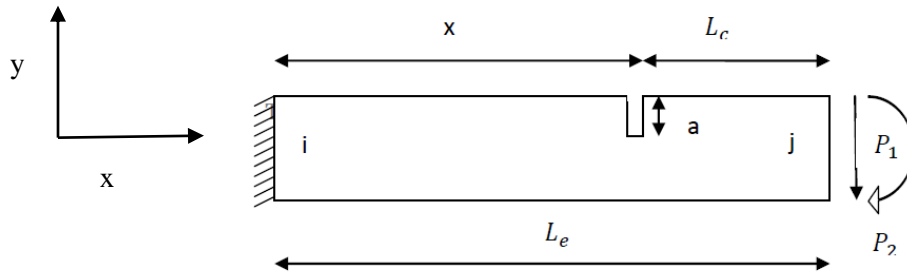


Figure 4-2 A regular cracked beam element which is subjected to shearing force and bending moment of rectangular cross-section area

According **Zheng (2004)**, due to the presence of the crack the additional strain energy is given by the following equation,

$$\pi = \int_A G dA_c \quad (4.30)$$

Where, G = strain energy release rate,

A_c = effective cracked area

The strain energy release rate is given by,

$$G = \frac{1}{E} [(\sum_{n=1}^2 K_{In})^2 + (\sum_{n=1}^2 K_{IIIn})^2 + (\sum_{n=1}^2 K_{IIIIn})^2] \quad (4.31)$$

K_I , K_{II} , K_{III} are the stress intensity factors for opening crack, sliding crack and tearing type cracks.

By considering the effect of shearing force and bending moment, the above equation becomes,

$$G = \frac{1}{E'} [(K_{I1} + K_{I2})^2 + (K_{II1})^2] \quad (4.32)$$

$$\begin{aligned} K_{I1} &= \frac{6P_1 L_c^2}{bh^2} \sqrt{\pi \xi F_I} \left(\frac{\xi}{h} \right) \\ K_{I2} &= \frac{6P_2}{bh^2} \sqrt{\pi \xi F_{II}} \left(\frac{\xi}{h} \right) \\ K_{II2} &= \frac{P_2}{bh^2} \sqrt{\pi \xi F_{II}} \left(\frac{\xi}{h} \right) \end{aligned} \quad (4.33)$$

Where, F_I and F_{II} are the correction factors for stress intensity factors.

$$F_I(s) = \sqrt{\frac{\tan \frac{\pi s}{2}}{\frac{\pi s}{2}}} \left[\frac{0.923 + 0.199 \left((1 - \sin \frac{\pi s}{2})^4 \right)}{\cos \frac{\pi s}{2}} \right] \quad (4.34)$$

$$F_{II}(s) = \frac{1.122 - 0.561s + 0.085s^2 + 0.180s^3}{\sqrt{1-s}} \quad (4.35)$$

Where $s = \frac{\xi}{h}$, ξ = crack depth during the process of penetration of the crack, which varies from zero to final depth.

Using Paris equation, $\delta_i = \frac{\partial \pi_c}{\partial P_i}$

$$C_{ij} = \frac{\partial \delta_i}{\partial P_j} = \frac{\partial^2 \pi_c}{\partial P_i \partial P_j}$$

$$C_{11} = \frac{2\pi}{E' b} \left[\frac{36L_c^2}{h^2} \int_0^{\frac{a}{h}} x F_1^2(x) dx + \int_0^{\frac{a}{h}} x F_{11}^2(x) dx \right]$$

$$C_{12} = \frac{72\pi L_c}{E' b h^2} \int_0^{\frac{a}{h}} x F_1^2(x) dx = C_{21}$$

$$C_{22} = \frac{72\pi}{E' b h^2} \int_0^{\frac{a}{h}} x F_1^2(x) dx$$

$$C_{ovl} = \begin{bmatrix} C_{11} & C_{12} \\ C_{21} & C_{22} \end{bmatrix}$$

The flexibility matrix for an intact tapered beam is given by,

$$C_{intact} = \begin{bmatrix} \frac{L_e^3(I_1+3I_2)}{2E(I_1^2+4I_1^2I_2^2+I_2^2)} & \frac{L_e^2(I_1+2I_2)}{E(I_1^2+4I_1^2I_2^2+I_2^2)} \\ \frac{L_e^2(I_1+2I_2)}{E(I_1^2+4I_1^2I_2^2+I_2^2)} & \frac{3L_e(I_1+I_2)}{E(I_1^2+4I_1^2I_2^2+I_2^2)} \end{bmatrix} \quad (4.36)$$

$$C_{total} = C_{ovl} + C_{intact} \quad (4.37)$$

Stiffness matrix ' K_c ' for cracked element is given as,

$$C_{total} = \begin{bmatrix} \frac{L_e^3(I_1+3I_2)}{2E(I_1^2+4I_1^2I_2^2+I_2^2)} + C_{11} & \frac{L_e^2(I_1+2I_2)}{E(I_1^2+4I_1^2I_2^2+I_2^2)} + C_{12} \\ \frac{L_e^2(I_1+2I_2)}{E(I_1^2+4I_1^2I_2^2+I_2^2)} + C_{21} & \frac{3L_e(I_1+I_2)}{E(I_1^2+4I_1^2I_2^2+I_2^2)} + C_{22} \end{bmatrix} \quad (4.38)$$

$$K_c = [L][C_{total}]^{-1}[L]^T \quad (4.39)$$

$$\text{Where, } [L] = \begin{bmatrix} -1 & 0 \\ L_e & -1 \\ 1 & 0 \\ 0 & 1 \end{bmatrix}, L_e = \text{Length of beam}$$

$[M]\ddot{u} + [K]u = 0$ is the equation of motion for an undamped free vibration analysis of the beam

which is reduced to

$$[K_c] - \omega^2 [M_e] = 0 \quad (4.40)$$

There will be no change in mass distribution due to the presence of crack.

A computer program is developed to perform all the necessary computations in MATLAB environment.

RESULTS AND DISCUSSION:

5.1. Introduction:

The dynamic and static behavior of a beam can be studied with its stiffness properties. Structural defects are origin for local flexibilities results deficiency in structural resistance. The presence of cracks in a structure results, changes in its stiffness. We can observe the changes in the local flexibilities Structural deficiencies like cracks give deficiencies in the local flexibilities. In this chapter the following contents are discussed,

1. Convergence study
2. Comparison with previous data
3. Results on the effects of various parameters on the vibration and buckling of intact and single cracked tapered beam are presented.

A MATLAB code is developed to calculate the natural frequencies and mode shapes of the tapered cantilever beam by using the Finite element method. The solutions thus obtained are compared with previously established results to check the accuracy of the lower four natural frequencies for various crack depths and various crack positions.

5.2. Numerical Problem for Intact Tapered Beam:

For numerical analysis a tapered beam is considered with the following properties:

Properties:

Length, $l=240\text{mm}$,

Width of the beam at fixed end, $b_1=12\times 10^{-2}\text{ m}$.

Depth of the beam at fixed end, $h_1=20 \times 10^{-2}$ m.

Density = 7860 Kg/m³

Modulus of elasticity, $E = 210$ GPa.

Poisson's Ratio $\gamma = 0.3$

Taper ratio's $\alpha=0.2$ and $\beta=1$

Where, $\alpha = \frac{h_1}{h_2}$ and $\beta = \frac{b_1}{b_2}$

b_2, h_2 are the breadth and the depth at the free end

5.2.1. Convergence Study

A graph is plotted between fundamental natural frequencies to the number elements. We can observe from fig. 5-1 that the frequency values are converging at minimum elements of 14

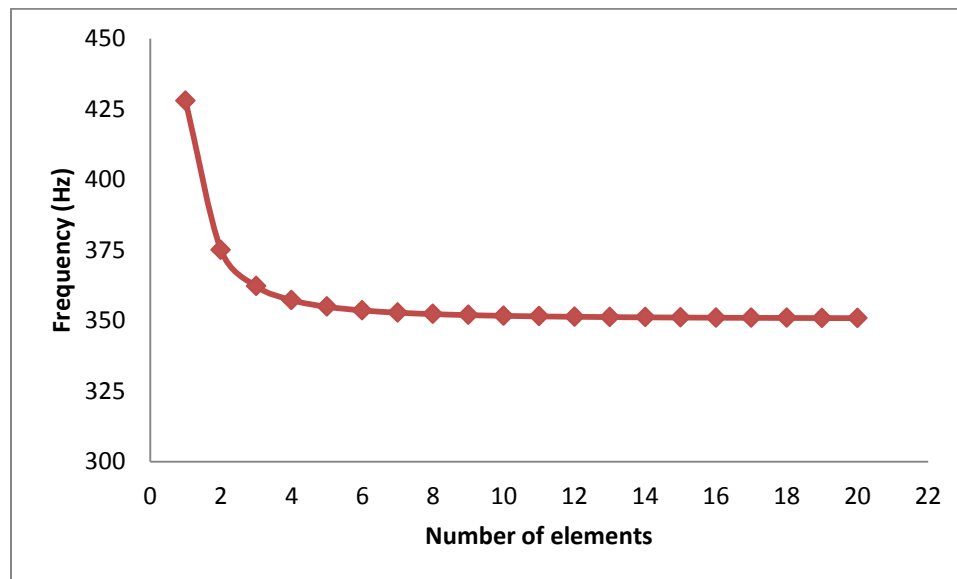


Figure 5-1 Convergence of fundamental frequency of an intact tapered cantilever beam

Though the frequency is converging at a minimum of 12 elements, we are considering 20 elements for more approximation

5.2.2. Comparison with Previous Studies:

The obtained frequency values are thus compared to Choudary *et al.* (1999) in Table 5.1. It is observed from the table 5-1, that the values obtained from the present study are in good agreement with the paper and the percentage error is acceptable.

Table 5-1 Comparison of frequencies of an intact tapered cantilever beam with previous studies

MODE	Natural Frequency (Hz)		% error
	Choudary et al.(2009)	Present analysis (FEM)	
MODE1	351.62	351.06	0.44
MODE2	1271.54	1289.17	1.38
MODE3	2925.31	3022.81	3.33

5.2.3. Effect of Taper Ratio on Frequency for an intact tapered beam:

The taper ratio factors are $\alpha = \frac{h_2}{h_1}$ and $\beta = \frac{b_2}{b_1}$, have the range from 0 to 1.

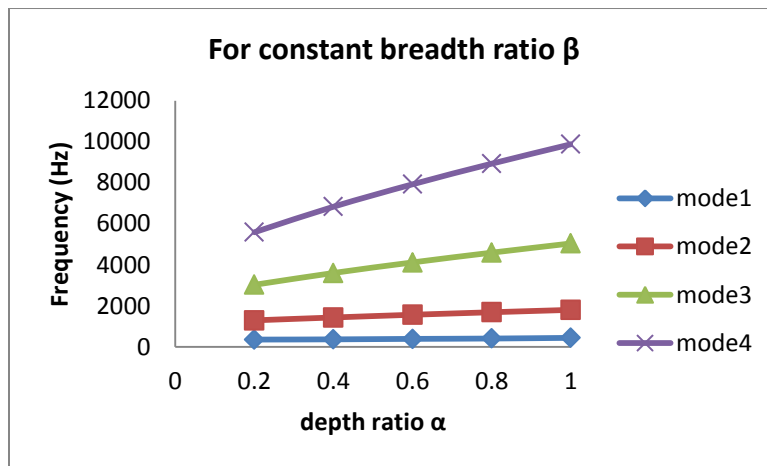


Figure 5-2 Effect of α on frequency for constant values of β

It is observed from fig. 5-2 that the frequency values are increasing rapidly for the depth ratio varying from 0.2 to 1, while the breadth ratio kept constant. More the mode of frequency more will be the increment.

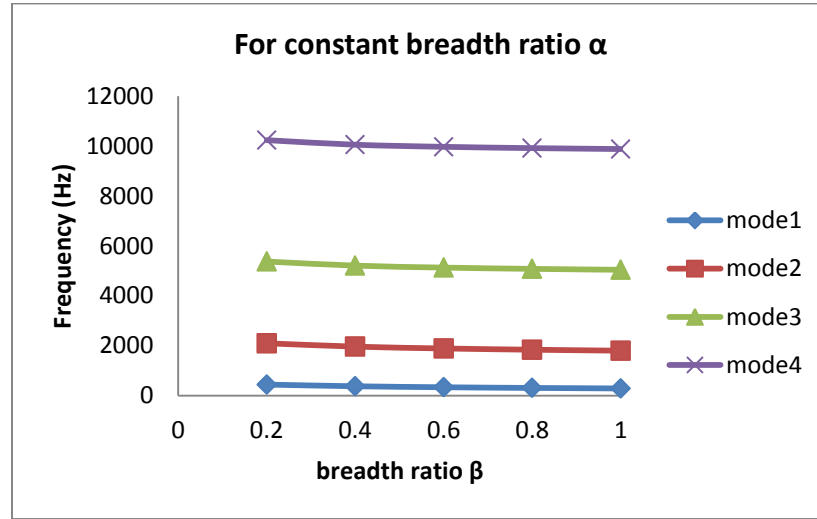


Figure 5-3 Effect of β on frequency for constant values of α

It is observed from fig. 5-3 that the frequency values are decreasing for the breadth ratio varying from 0.2 to 1, while the depth ratio is constant.

For the same rate of increase in the tapering, frequencies are increasing rapidly for depth ratio α , whereas the breadth ratio β has a detrimental effect.

5.3. Effect depth ratio on buckling load for an intact tapered beam:

To study the effect of depth ratio factors on the buckling loads, a graph is plotted between buckling load and different values of depth ratio α . The beam is considered to be of constant thickness. The graph is shown in the fig. 5-4.

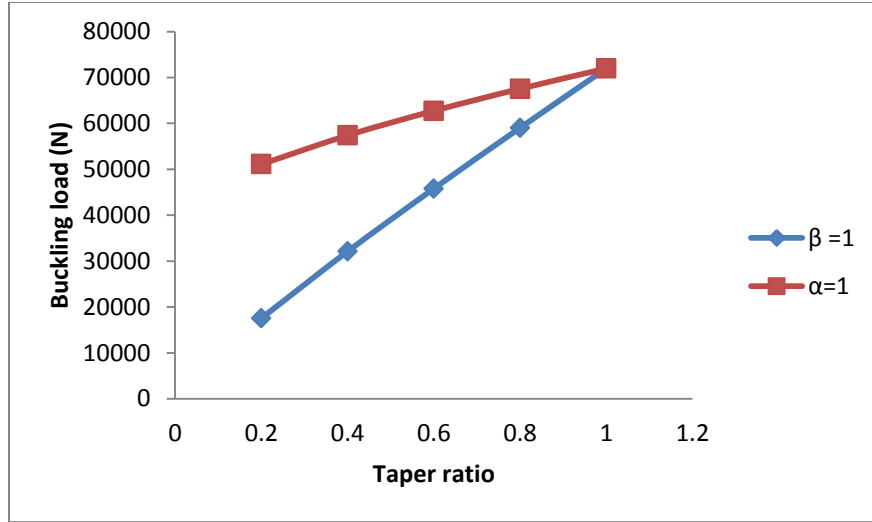


Figure 5-4 Effect depth ratio on buckling load

It is observed that from fig. 5-4, the buckling load values increase more rapidly with an increase in depth ratio α than the depth ratio β .

5.4. Numerical Problem for Tapered Beam with Single Transverse Crack:

For numerical analysis of the single cracked tapered beam is considered with the following properties:

Properties

Length, $L=240\text{mm}$,

Width of the beam at fixed end, $b_1=12\times 10^{-2}\text{ m}$.

Depth of the beam at fixed end, $h_1=20\times 10^{-2}\text{ m}$.

Density = 7860 Kg/m^3

Modulus of elasticity, $E = 210\text{ GPa}$.

Poisson's Ratio $\gamma = 0.3$

Taper ratio's $\alpha=0.2$ and $\beta=1$

Where, $\alpha = \frac{h_1}{h_2}$ and $\beta = \frac{b_1}{b_2}$

b_2, h_2 is the breadth and the depth at the free end

Crack location $\chi = 0.5$, $a/h_c=0.288$

Where, 'a' is cracked depth and 'h_c' is the depth at the corresponding crack section.

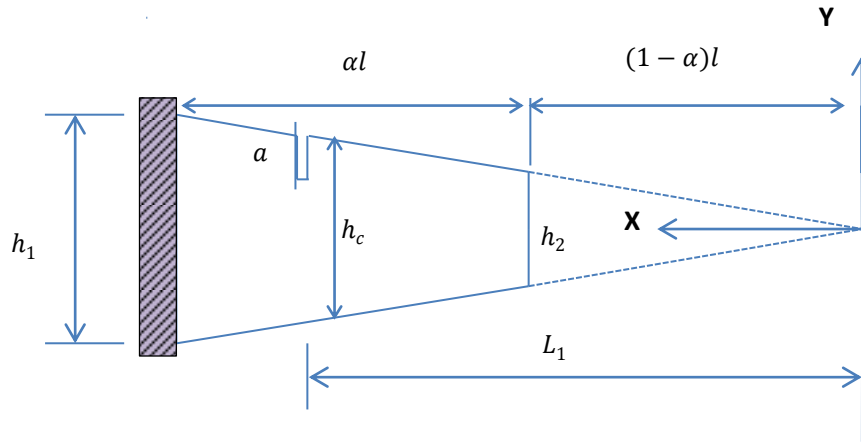


Figure 5-5 Geometrical representation of crack

5.4.1. Convergence study:

A graph is plotted between fundamental natural frequencies to the number elements.

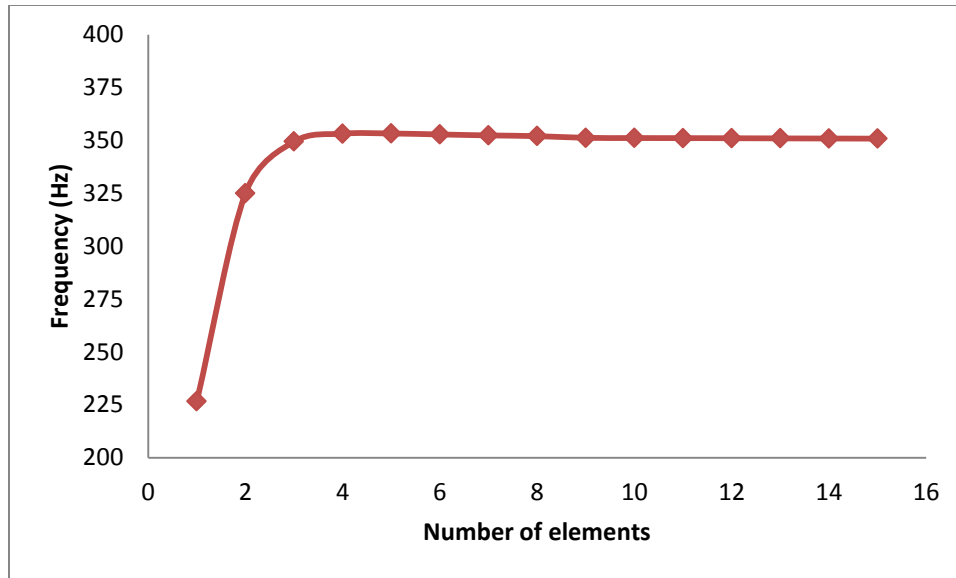


Figure 5-6 Convergence of fundamental frequency of a single cracked tapered cantilever beam

It is observed from fig. 5-6 that the frequency values are converging at minimum elements of 12. Initially the fundamental frequency is decreased since the effect of crack in single element is more than more in number of elements. And also it is observed from figure 5-6 that from the element number four onwards the frequency got stabilized and is converging for the number of elements 12.

Though the frequency is converging at a minimum of 12 elements, it is considered 15 elements for more approximation.

5.4.2. Comparison with Previous Studies:

The obtained frequency values are thus compared to Choudary et al. (2009) in table 5-2

Table 5-2 Comparison of natural frequencies of a single cracked tapered cantilever beam with previous studies

MODE	Natural Frequency		% error
	Choudary et al.(2009)	Present analysis FEM	
MODE1	348.36	349.13	0.22
MODE2	1230.03	1265.44	2.87
MODE3	2923.00	3023.74	3.44

It is observed from the table 5-2 that the values obtained from the present study are very nearer and the percentage error is acceptable.

Table 5-3 Comparison of frequencies with previous studies for different values of crack depth and location

	Crack		Present analysis (FEM)		Choudary et al. (2009)	
	Location χ	a/h _c	MODE1	MODE2	MODE1	MODE2
Case 1	0.5	0.288	349.13	1265.44	348.36	1230.03
Case2	0.6	0.292	346.01	1274.66	344.38	1242.13
Case3	0.95	0.399	322.52	1207.10	307.34	1156.18
Case4	0.99	0.5	293.90	1112.09	292.07	1097.61

It is observed from table 5-3 that for different combinations of crack depth and locations the frequencies are compared with to Choudary et al. (2009). The frequency values are compared and tabulated below for different values of crack depth and location of crack.

5.4.3. Effect of Crack on frequencies at Various Locations in Tapered Beam for Fixed-Free Boundary Condition

The Non-dimensional natural frequencies are computed for the tapered cantilever beam for a crack considered at relative locations (L_1/l) which can be represented by ' χ ' varies from 0.2 to 0.9 with relative crack depths (a/h_c) 0.1, 0.3 and 0.5 for constant depth and breadth ratio. The free vibration results are plotted in Fig. 5.6, 5.7, 5.8 and 5.9 for frequency mode 1,2,3 and 4 respectively.

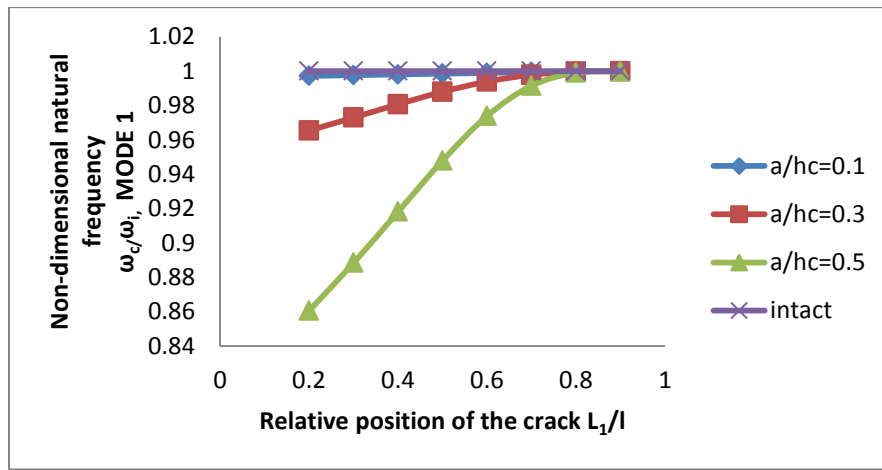


Figure 5-7 Variation of first mode natural frequency of cracked tapered cantilever beam for different values of χ and a/h_c

It is observed from fig. 5-7 that, the first mode of natural frequency reduced approximately 0.27%, 3.45% and 13.93% for relative crack depths 0.1, 0.3 and 0.5 respectively for location factor 0.2 from fixed end. And for the crack location factor 0.9, from the fixed end, the non-dimensional frequencies are almost same as intact tapered beam. This implies that the non-dimensional frequency for first mode is maximum at free end compared to all other relative locations for any depth of the crack.

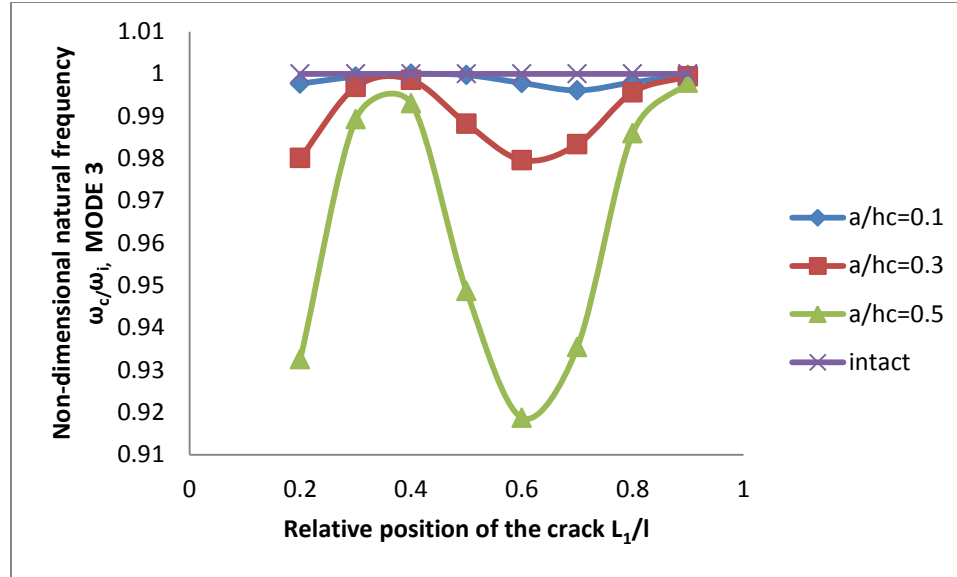


Figure 5-8 Variation of second mode natural frequency of cracked tapered cantilever beam for different values of χ and a/h_c

For the second mode of frequency, it is observed from fig. 5-7 that for the crack location factor 0.2, the natural frequency reduced approximately 0.23%, 1.99% and 6.74% for relative crack depths 0.1, 0.3 and 0.5 respectively. And the maximum drop in the non-dimensional frequencies. 0.21%, 2.03%, 8.13% located for a crack location factor of 0.6 from the fixed end.

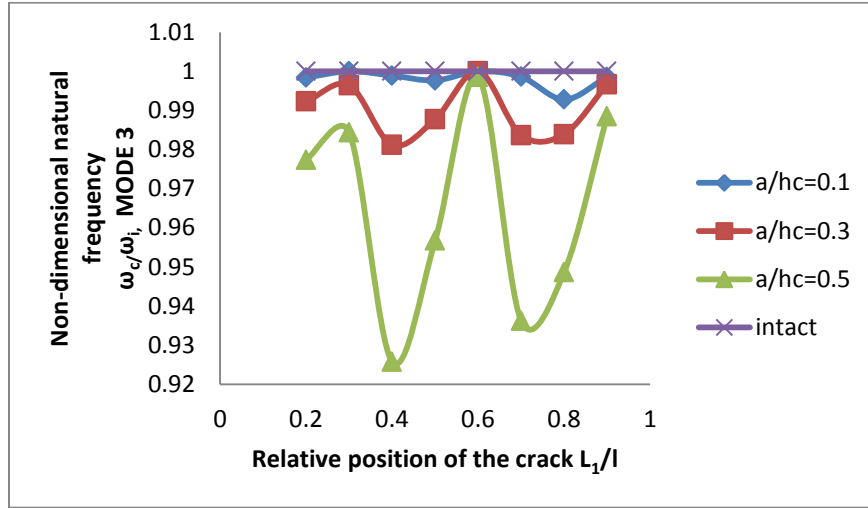


Figure 5-9 Variation of third mode natural frequency of cracked tapered cantilever beam for different values of χ and a/h_c

For the third mode of frequency, it is observed from fig. 5-9 that for the crack location factor 0.2, the natural frequency reduced approximately 0.15%, 0.76% and 2.26% for relative crack depths 0.1, 0.3 and 0.5 respectively. And for the crack location factor 0.9 from the fixed end the non-dimensional frequencies are reduced by 0.14%, 0.33% and 1.15%. The maximum drop in the non-dimensional frequencies 0.11%, 1.87% and 7.42% located for a crack location factor of 0.4 from the fixed end.

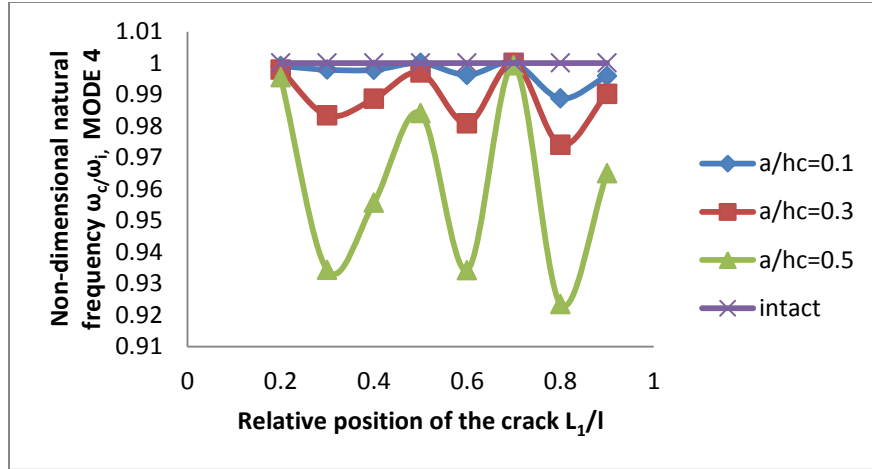


Figure 5-10 Variation of fourth mode natural frequency of cracked tapered cantilever beam for different values of χ and a/h_c

For the fourth mode of frequency, it is observed from fig. 5-10 that for the crack location factor 0.2, the natural frequency reduced approximately 0.09%, 0.20% and 0.44% for relative crack depths 0.1, 0.3 and 0.5 respectively. And for the crack location factor 0.9 from the fixed end the non-dimensional frequencies are reduced by 0.41%, 0.97% and 3.5%. The maximum drop in the non-dimensional frequencies 1.12%, 2.59% and 7.65% located for a crack location factor of 0.81 from the fixed end.

5.4.4. Effect of Taper Ratio on Frequency of a single cracked tapered beam:

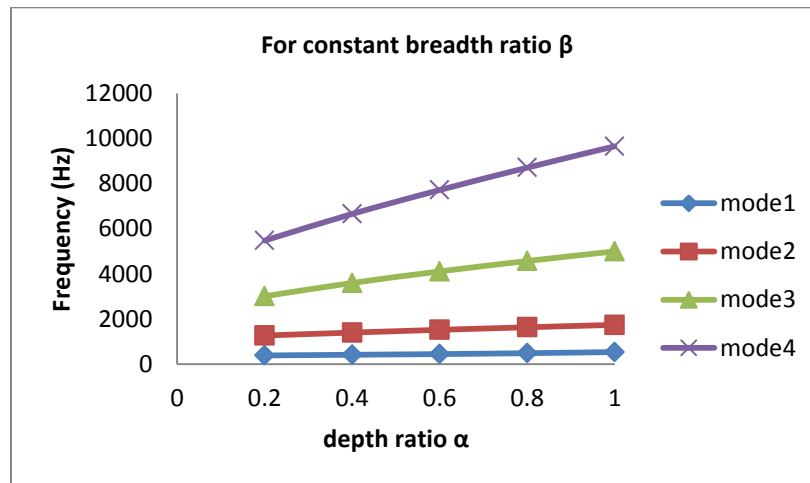


Figure 5-11 Effect of β on frequency for constant values of α

It is observed from fig. 5-11 that the frequency values are increasing rapidly for the depth ratio varying from 0.2 to 1, while the breadth ratio kept constant. More the mode of frequency more will be the increment.

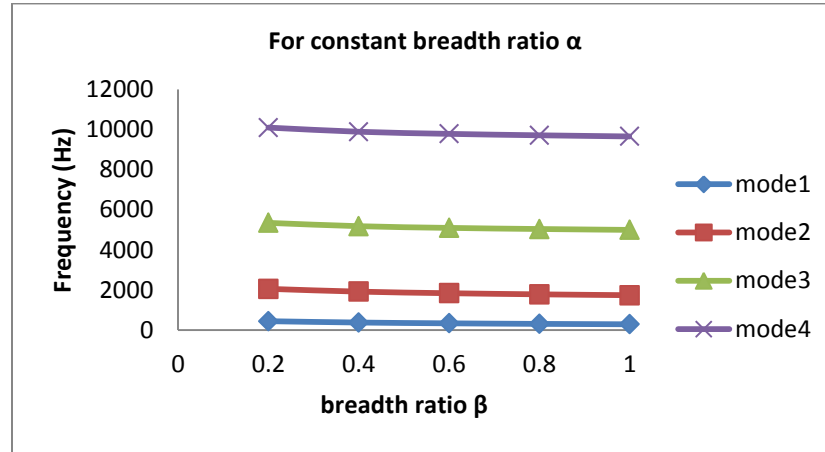


Figure 5-12 Effect of β on frequency for constant values of α

It is observed from fig. 5-12 that the frequency values are decreasing for the breadth ratio varying from 0.2 to 1, while the depth ratio is constant. More the mode of frequency, more will be the increment.

For the same rate of increase in the tapering, frequencies are increasing rapidly for depth ratio α , whereas the breadth ratio β has a detrimental effect.

5.5. Buckling of beam subjected to single crack for different end conditions of the beam

The Non-dimensions buckling loads are computed for the tapered beam for a crack considered at relative locations (L_1/l) which can be represented by ' χ ' which varies from 0.2 to 0.9 with relative crack depths (a/h_c) 0.1, 0.2, 0.3, 0.4 and 0.5 for different end conditions.

5.5.1. Fixed free beam:

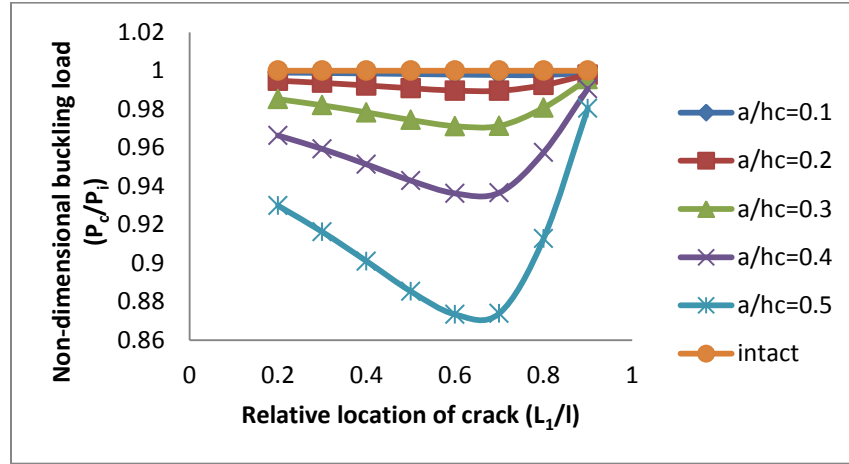


Figure 5-13 Variation of non-dimensional buckling load (P_c/P_i) with respect to relative location of crack (L_1/l) for different relative crack depths for Fixed-Free beam

It is observed from fig. 5-13 that for the crack location factor 0.2, the buckling loads reduce approximately 0.1%, 0.5%, 1.5%, 3.3% and 7.0% for relative crack depths 0.1, 0.2, 0.3, 0.4 and 0.5 respectively. And for the crack location factor 0.9 from the fixed end the non-dimensional buckling loads are reduced by only 0.1%, 0.2%, 0.44%, 0.93% and 1.95% for relative crack depths 0.1, 0.2, 0.3, 0.4 and 0.5 respectively. This implies that the non-dimensional buckling loads for a fixed-free beam maximum at free end compared to all other relative depths. This implies due to the maximum bending moment cause by the buckling load. This is due to the fact that higher bending moment near the fixed end of a fixed-free beam results in the larger release of strain energy in the section due to a crack. Due to a larger release in strain energy, the beam becomes more flexible; hence there is a maximum drop of buckling load. As in a tapered beam the cross section increased from the free end to fixed end, for a particular location on the span subjects to minimum buckling load due to the combined effect of strain energy and taper variation. These results for a location factor of 0.65, the buckling loads are minimum such as 0.1%, 1%, 3%, 6.5% and 13% for relative crack depths 0.1, 0.2, 0.3, 0.4 and 0.5 respectively.

5.5.2. Hinged-Hinged beam:

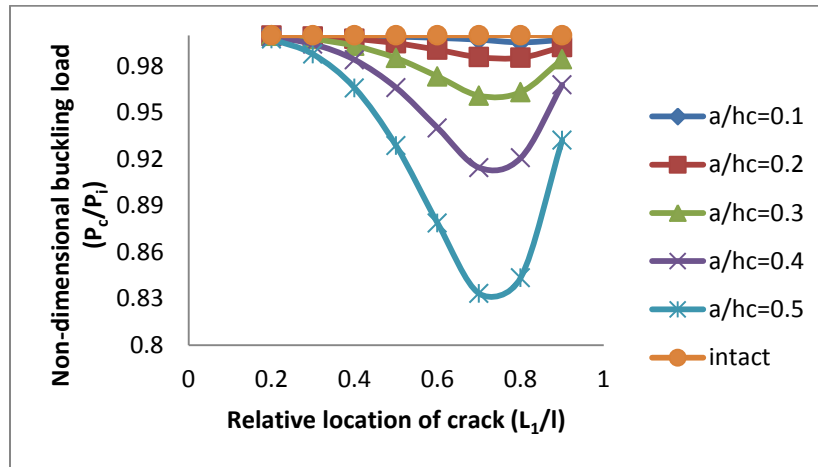


Figure 5-14 Variation of non-dimensional buckling load (P_c/P_i) with respect to relative location of crack (L_1/l) for different relative crack depths for Hinged-Hinged beam

It is observed from fig. 5-14 that for the crack location factor 0.2, the buckling loads reduce approximately 0%, 0.02%, 0.05%, 0.16% and 0.24% for relative crack depths 0.1, 0.2, 0.3, 0.4 and 0.5 from the larger section respectively. And for the crack location factor 0.9 from the larger section the non-dimensional buckling loads are reduced by 0.3%, 0.75%, 1.55%, 3.2% and 6.77% for relative crack depths 0.1, 0.2, 0.3, 0.4 and 0.5 respectively. This implies that the non-dimensional buckling loads for a hinged- hinged beam maximum at free end compared to the fixed end. This implies due to the unsymmetrical bending moment cause by the buckling load. Due to a larger release in strain energy, the beam becomes more flexible, hence there is a maximum drop of buckling load. In a uniform beam with hinged- hinged end conditions, the maximum drop of load will be in the middle of the span. As in a tapered beam the cross section increased from the smaller end to larger end. This is due to the fact that higher bending moment at the middle of the span of a hinged-hinged beam results in the larger release of strain energy in

the section due to a crack. For a particular location on the span subjects to minimum buckling load due to the combined effect of strain energy and taper variation. This result, for a location factor of 0.78 from the larger end, the buckling loads are minimum such as 0.28%, 1.41%, 3.9%, 8.54% and 16.67% for relative crack depths 0.1, 0.2, 0.3, 0.4 and 0.5 respectively.

5.5.3. Fixed–Fixed beam

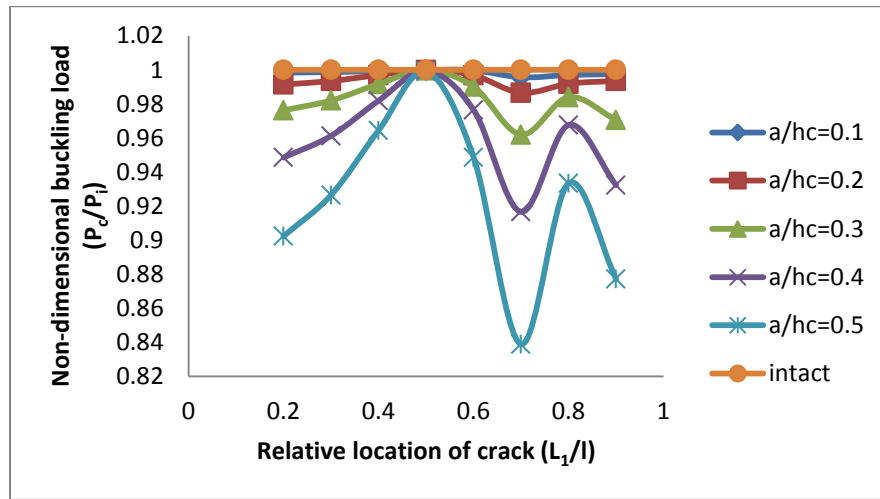


Figure 5-15 Variation of non-dimensional buckling load (P_c/P_i) with respect to relative location of crack (L_1/l) for different relative crack depths for Fixed-Fixed beam

It is observed from fig. 5-15 that for the crack location factor 0.2 from the larger end, the buckling loads reduce approximately 0.16%, 0.86%, 2.37%, 5.14% and 9.77% for relative crack depths 0.1, 0.2, 0.3, 0.4 and 0.5 respectively. And for the crack location factor 0.9 from the fixed end the non-dimensional buckling loads are reduced by 0.25%, 0.65%, 2.94%, 6.77% and 12.28% for relative crack depths 0.1, 0.2, 0.3, 0.4 and 0.5 respectively. This implies that the non-dimensional buckling loads for a fixed-fixed beam maximum at the larger end compared to the smaller end. This implies due to the unsymmetrical bending moment cause by the buckling load. Due to a larger release in strain energy, the beam becomes more flexible, hence there is a

maximum drop of buckling load. In a uniform beam with fixed- fixed end conditions, the maximum drop of load will be in the middle of the span. As in a tapered beam the cross section increased from the smaller end to a larger end. This is due to the fact that higher bending moment at the middle of the span of a fixed-fixed beam results in the larger release of strain energy in the section due to a crack. For a particular location on the span subjects to minimum buckling load due to the combined effect of strain energy and taper variation. This result, for a location factor of 0.7 from the larger end, the buckling loads are maximum such as 0.44%, 1.35%, 3.80%, 8.34% and 16.1% for relative crack depths 0.1, 0.2, 0.3, 0.4 and 0.5 respectively. And, for a location of 0.5 from the larger end the buckling loads are minimum such as 0.0%, 0.01%, 0.02%, 0.05% and 0.10 % for relative crack depths 0.1, 0.2, 0.3, 0.4 and 0.5 respectively.

5.5.4. Fixed-Hinged beam

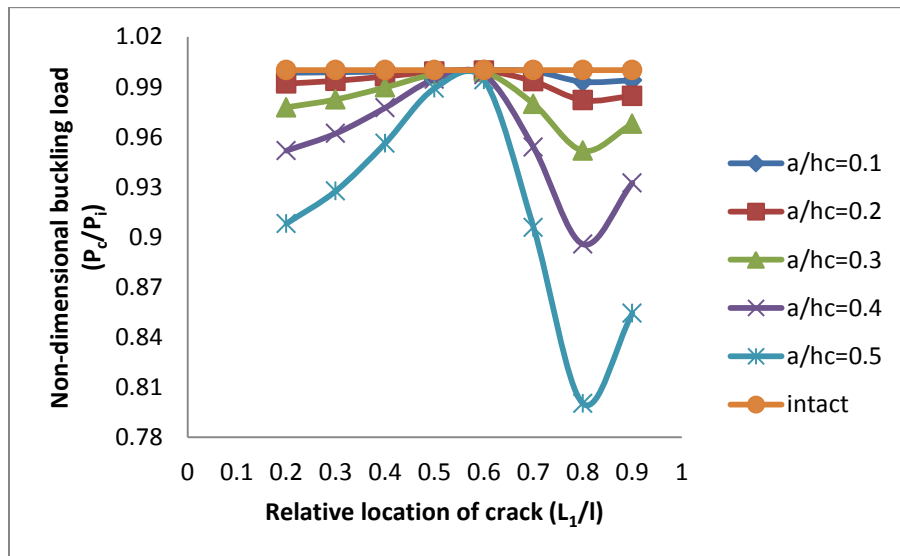


Figure 5-16 Variation of non-dimensional buckling load (P_c/P_i) with respect to relative location of crack (L_1/l) for different relative crack depths for Fixed-Hinged beam

It is observed from fig. 5-16 that for the crack location factor 0.2 from the larger end, the buckling loads reduce approximately 0.15%, 0.81%, 2.22%, 4.82% and 9.19% for relative crack

depths 0.1, 0.2, 0.3, 0.4 and 0.5 respectively. And for the crack location factor 0.9 from the fixed end the non-dimensional buckling loads are reduced by 0.61%, 1.55%, 3.21%, 6.76% and 14.57% for relative crack depths 0.1, 0.2, 0.3, 0.4 and 0.5 respectively. This implies that the non-dimensional buckling loads for a fixed-fixed beam maximum at the larger end compared to the smaller end. This implies due to the unsymmetrical bending moment cause by the buckling load. Due to a larger release in strain energy, the beam becomes more flexible, hence there is a maximum drop of buckling load. In a uniform beam with fixed- hinged end conditions, the maximum drop of load will be towards the free end. As in a tapered beam the cross section increased from the smaller end to a larger end. This is due to the fact that higher bending moment nearer the hinged end of the span of a fixed-hinged beam results in the larger release of strain energy in the section due to a crack. For a particular location on the span subjects to minimum buckling load due to the combined effect of strain energy and taper variation. This result, for a location factor of 0.58 from the larger end, the buckling loads are maximum are equivalent to the intact beam. And, for a location of 0.81 from the larger end the buckling loads are minimum such as 0.7%, 1.8%, 4.83%, 10.4% and 19.97 % for relative crack depths 0.1, 0.2, 0.3, 0.4 and 0.5 respectively.

5.6. Effect taper ratio on buckling load of a single cracked tapered beam:

To study the effect of depth ratio factors on the buckling loads, a graph is plotted between buckling load and different values of depth ratio α . The beam is considered to be of constant thickness. The graph is shown in the fig. 5-17.

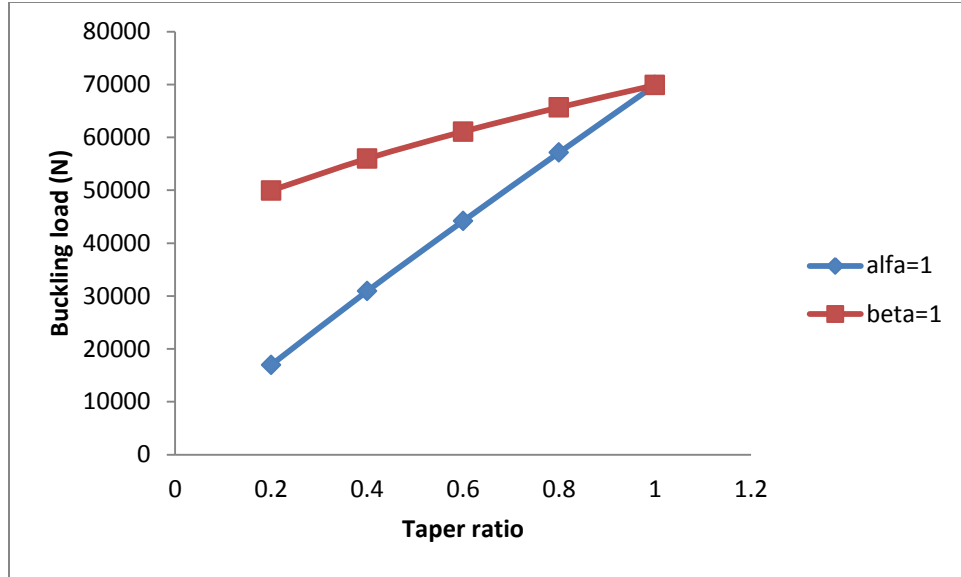


Figure 5-17 Effect of taper ratio on buckling load for single cracked tapered beam

It is observed that from fig. 5-17, the buckling load values increase more rapidly with increase in depth ratio α than the depth ratio β .

CONCLUSION AND FUTURE WORK

6.1. Conclusion

Free vibration and buckling analysis of a tapered beam subjected to a transverse crack has been carried out using Finite element method in Matlab environment. The following observations are concluded from the present study,

- Mathematical formulation for free vibration and buckling analysis of a tapered beam with transverse open edge crack is presented.
- Free vibration frequencies for both intact and single cracked tapered beams increase with increase in depth ratio (α) whereas the breadth ratio (β) has a detrimental effect. This is a very useful concept that can be used in structures or machine members where strength to weight ratio is important to be considered for minimal weight and highest strength, simultaneously increasing the fundamental frequency.
- The natural frequencies for a single cracked taper beam are influenced by crack depth, location of the crack and taper ratio.
- In a cracked tapered cantilever beam, the first mode of frequency has a maximum drop at the fixed end; the second mode of frequency has a maximum drop for a location factor of 0.6 from the fixed end. Similarly, the third and fourth mode of frequencies has a maximum drop at a location factor of 0.4 and 0.81 from the fixed ends respectively.
- Buckling loads for both intact and single cracked beam s increase rapidly with increase in the depth ratio α than breadth ratio β .

- For a Fixed-Free tapered beam subjected to a single transverse crack, the maximum drop in the buckling load is in the location factor of 0.65 from the fixed end. This is due to the combine effect of strain energy and tapering effect.
- For a Hinged-Hinged tapered beam subjected to a single transverse crack, the maximum drop in the buckling load is in the location factor of 0.78 from the larger end.
- For a Fixed-Fixed tapered beam subjected to a single transverse crack, the maximum drop in the buckling load is in the location factor of 0.7 from the fixed end.
- For a Fixed-Hinged tapered beam subjected to a single transverse crack, the maximum drop in the buckling load is in the location factor of 0.81 from the fixed end.
- With the study of vibration of the tapered beam, possible detection of the crack can estimated.

6.2. Scope of the Future Work

- An experimental study can be carried out for free vibration and buckling behavior of tapered cracked beam with transverse crack.
- Present study can be further extended to Dynamic stability.

REFERENCES

1. Achawakorn, K. and Jearsiripongkul, T.(2012), “Vibration Analysis of Exponential Cross-Section Beam Using Galerkin’s Method”, *International Journal of Applied Science and Technology*, Vol. 2 No. 6
2. Auciello, N.M.(2013), “Dynamic analysis of rotating tapered Rayleigh beams using two general approaches”, *Electronic International Interdisciplinary Conference September*, 2. – 6.
3. Bayat, M., Pakar, I. and Bayat, M.(2011), “Analytical study on the vibration frequencies of tapered beams”, *Latin American Journal of Solids and Structures* 8, 149-162.
4. Bazoune, A., Khulief Y.A., Stephen, N.G. and Mohiuddin, M.A., (2001), “Dynamic response of spinning tapered Timoshenko beams using modal reduction”, *Finite Elements in Analysis and Design*, 37, 199-219.
5. Behzad, M., Meghdari, A. and Ebrahimi, A., (2005) “A new approach for vibrational analysis of a cracked beam”, *international journal of engineering*, Vol. 18, No. 4, 319.
6. Chaudhari, T.D. and Maiti, S.K., (1999), “Modeling of transverse vibration of beam of linearly variable depth with edge crack”, *Engineering Fracture Mechanics* 63, 425-445.
7. Cheng, Y., Zhigang Y., Xun W. and Yuan, Y.(2011), “Vibration analysis of a cracked rotating tapered beam using the p-version finite element method”, *Finite Elements in Analysis and Design* 47, 825–834
8. Daniel J. Marquez-Chisolm, “Natural frequencies and mode shapes of non-linear uniform cantilever beam”, *AFIT/GAE/ENY/06-S06*.
9. De Rosa, M. A. and Auciello, N. M.(1996), “Free vibration of tapered beams with flexible ends”, *Computers & Structures* Vol. 60, No 2, 197-202.

10. Dhyai Hassan Jawad, "Free vibration and buckling behavior of tapered beam by finite element method", *Journal of Babylon University/Engineering Sciences/ No.(3)/ Vol.(21)*.
11. Gupta, Arvind K. (1985), "Vibration of Tapered beam", *J. Struct. Eng.* 1985.111:19-36.
12. Karaagac, C., Ozturk, H. and Sabuncu, M.(2009), "Free vibration and lateral buckling of a cantilever slender beam with an edge crack: Experimental and numerical studies", *Journal of Sound and Vibration* 326, 235–250.
13. Kukla, S. and Zamojska, I.(1994), "Free vibrations of a system of non-uniform beams coupled by elastic layers", *Journal of Theoretical and Applied Mechanics*, 3, 32, 581-590.
14. Mazanoglu, K., Yesilyurt, I. and Sabuncu, M.(2009) "Vibration analysis of multiple-cracked non-uniform beams", *Journal of Sound and Vibration*", 320, 977–989.
15. Radhakrishnan, V. M.(2004), "Response of a Cracked Cantilever Beam to Free and Forced Vibrations", *Defence Science Journal*, Vol. 54, No. 1, 31-38.
16. Rezaee, M. and Hassannejad, R.(2010), "Damped free vibration analysis of a beam with a fatigue crack using energy balance method", *International Journal of the Physical Sciences* Vol. 5(6), pp. 793-803,.
17. Trahair, N.S.(2014), "Bending and buckling of tapered steel beam structures", *Engineering Structures*, 59, 229–237
18. Wang, H.C. and Worley, W.J. (1996), "Tables of natural frequencies and nodes for transverse vibration tapered beams", *Prepared under Grant No. NsG-434 by UNIVERSITY OF ILLINOIS Urbana*.